Supplemental Materials

Human HELQ regulates DNA end resection at DNA double-strand breaks and stalled replication forks

LEGENDS FOR SUPPLEMENTARY FIGURES

Figure S1. Fusion tag knock-in and gene knock-out cell lines (related to Figure 1). A. Schematic shows the location of the EGFP- fusion tag at the N terminal of endogenous Ku70 introduced by CRISPR/Cas9 technology and verification by western blotting. B. HELQ KO cells generated by CRISPR/Cas9 with the indicated gRNA were verified by sequencing (left) or western blotting (right). C. Schematic shows the location of the SFB- fusion tag at the N terminal of endogenous HELQ introduced by CRISPR/Cas9 technology and verification by western blotting.

Figure S2. HELQ promotes ssDNA formation (related to Figure 2 and Figure 3). A. CtIP KO cells generated by CRISPR/Cas9 with the indicated guide RNA were verified by sequencing (left) and western blotting (right). B-C. RPA2 phosphorylation was detected by western blotting after the indicated cells were treated with 2 μM CPT (B) or 10 μM etoposide (ETO, C) for the indicated times. D. The cells were incubated with BrdU for 24 h, then treated with 10 μM ETO for the indicated times, fixed and then stained with BrdU and γH2AX antibodies under native conditions. Representative images (left) and the quantification of the average number of BrdU foci per γH2AX positive cell (right) are shown. Scale bar = 10 μm. E-G. U2OS (WT), HELQ KO cells (#2, E and #3, F) or HELQ KO #1 cells expressing exogenous EGFP-HELQ (G) were treated with CPT followed by RPA2 phosphorylation analysis by western blotting with the indicated antibodies. H. HELQ KO #1 cells expressing exogenous FLAG-HELQ were treated with CPT (2 μM, 1 h) and subjected to RPA2 foci formation analysis. Representative images (top) and the quantification of the average number of RPA2 foci per cell (bottom) are shown. Western blots show the expression of FLAG-HELQ, with β-actin as a loading control. Scale bar = 5 μm. I. EGFP-HR repair assays were performed in U2OS cells (WT) and HELQ KO cells expressing indicated shRNAs. Diagram shows the EGFP-HR DSB repair reporter (Left). Western blots show silencing of indicated protein, with β-actin as a loading control (Right). The data represent the means ± SD of three independent experiments. $^{****}P < 0.0001$, $^{**}P < 0.01$, n.s.: not significant. Mann-Whitney test was used in D and H. Student's t-test was used in I.

Figure S3. Analysis of HELQ biochemical activity in *vitro* (related to Figure 4). A. Purified proteins used in this study detected by Coomassie blue staining after SDS-PAGE. B. Resection assay, as in Figure 4A and 4B, was performed using the indicated proteins. C. 3'-overhang DNA substrate

（7 nM） was incubated with purified EXO1（15 nM） in the presence or absence of HELQ（40 nM) for 8 minutes and the products were resolved on a 0.8% agarose gel. D and E. Representative native gels of DNA unwinding assay using the indicated proteins and a 3'-overhang DNA substrate. F. Protein sequence alignment of HELQ homologues from different species. G. A DNA unwinding assay was performed as in D and E, using HELQ K587A protein. H. Electrophoretic mobility shift assays, as in Figure 4E, were performed using 3'-overhang DNA substrate. A represent gel and quantification of DNA binding capacity is shown. Error bars represent means ± SD of three independent experiments. ***$P < 0.001$, **$P < 0.01$. Student's t-test.

Figure S4. HELQ is involved in fork protection (related to Figure 5). A. U2OS cells treated with or without (No) 2 mM HU for 4 h before PLA assays were performed with the indicated antibodies. Left, representative PLA foci (green). Right, the quantitation of PLA foci per cell. Scale bar = 10 μm. B. U2OS (WT) and HELQ KO #2 cells were treated with indicated drugs (HU and CPT for 4 h) followed by RPA2 phosphorylation analysis by western blotting. C and D. Western blotting was performed using indicated antibodies to show silencing of indicated protein by shRNA in U2OS or HELQ KO #1 cells. The cells in S4C and S4D were used for the analysis shown in Figures 5D and 5E, respectively. E. The RAD51-nascent DNA (EdU) interaction was analyzed by PLA in U2OS cells (WT) and HELQ KO #1 cells expressing the indicated shRNAs (BLM and RADX) after HU treatment (2 mM, 4 h). Representative images and quantification of the average number of PLA foci per nucleus are shown. Scale bar = 5 μm. F. Western blotting was performed using the indicated antibodies to show the extent of shRNA-mediated BLM (top) and RADX (bottom) silencing in U2OS or HELQ KO #1 cells. The cells were used for the analysis shown in Figures 5G and S4E. In panel A and E, the data represent the means ± SD from at least three independent experiments. ****$P < 0.0001$. Mann-Whitney test.

Figure S5. The roles of HELQ variants in DSB repair and fork protection (related to Figure 6). A. Time-lapse imaging of EGFP-HELQ variants in U2OS cells before and after microirradiation. The red line marks the damage region. Scale bar = 5 μm. B. HR repair assay was performed in EGFP-HR-HELQ KO cells expressing the indicated HELQ variants. C. HCT116 cells (WT) and HCT116 cells expressing vector control (Ctrl) or the indicated HELQ variants with endogenous HELQ silenced by expressing Cas9 and a single guide RNA (sgRNA) targeting the HELQ gene were treated with 2 mM HU for 4 h and then subjected to metaphase spread assays. Representative metaphase spreads are shown, with arrows indicating chromosomal aberrations and the corresponding scatter plot of chromosomal aberrations per cell. Western blots show the expression of the indicated proteins, with β-actin as a loading control. The data represent the means ± SD from at least three independent experiments. ****$P < 0.0001$. **$P < 0.01$, *$P < 0.05$, n.s.: not significant. Student's t-test was used in B. Mann-Whitney test was used in C.

Figure S6. Western blotting was performed using the indicated antibodies to show the extent of shRNA-mediated silencing of the indicated proteins (related to Figure 7).

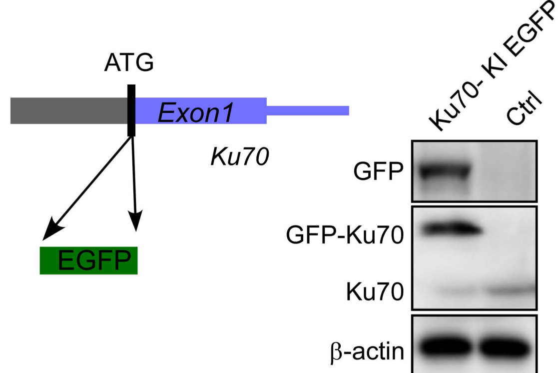

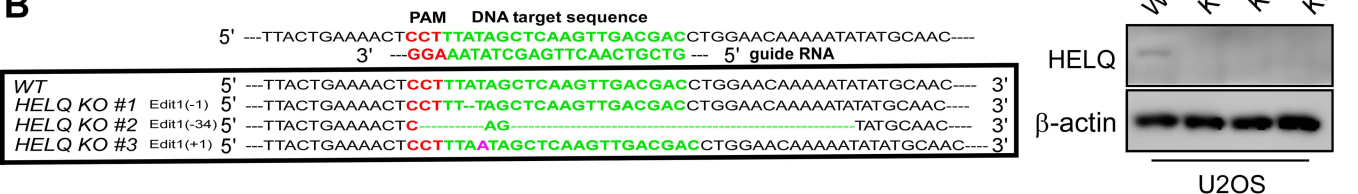

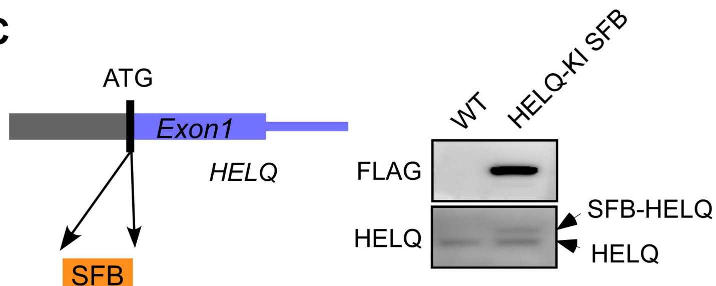

Figure S1

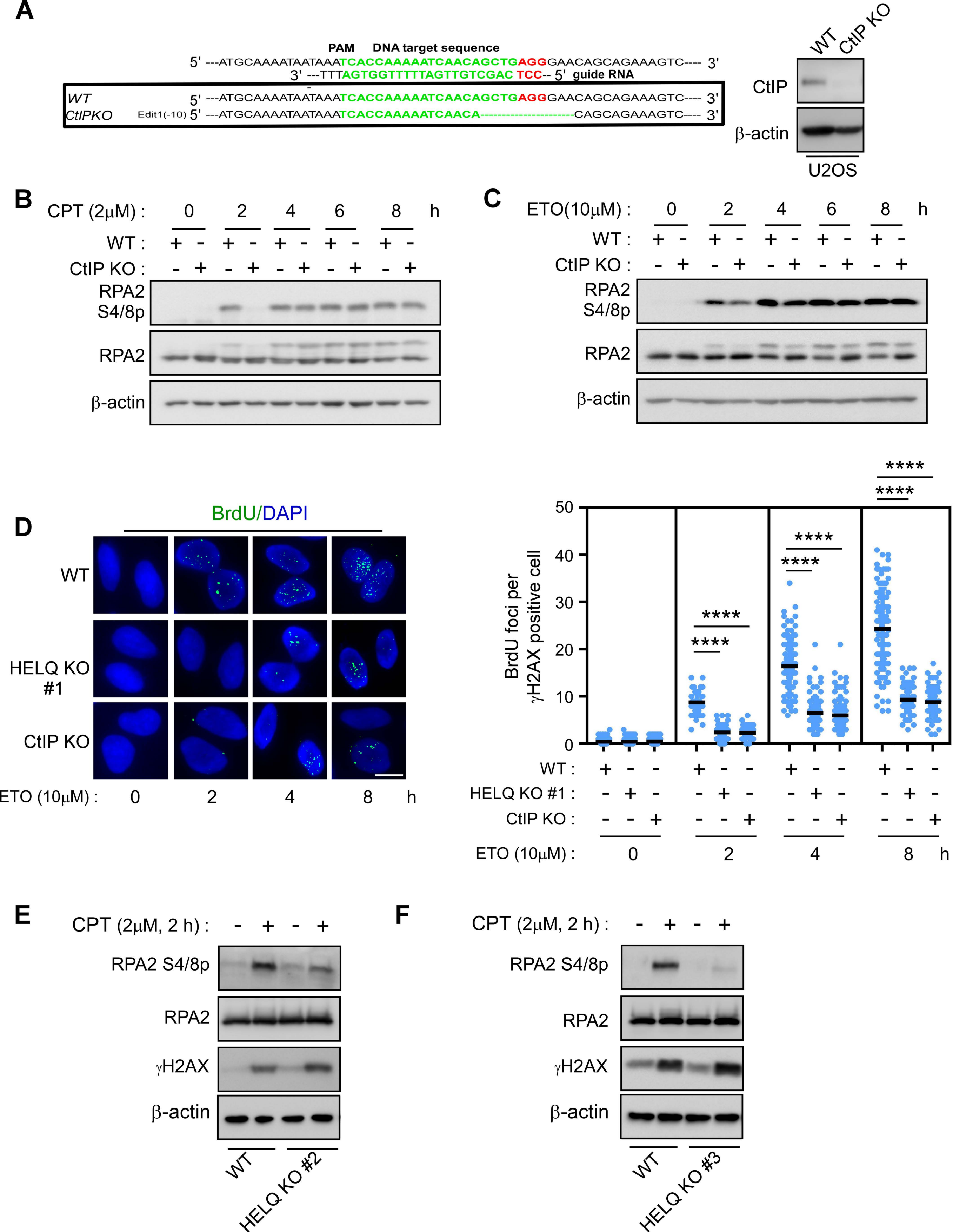

FigureS2

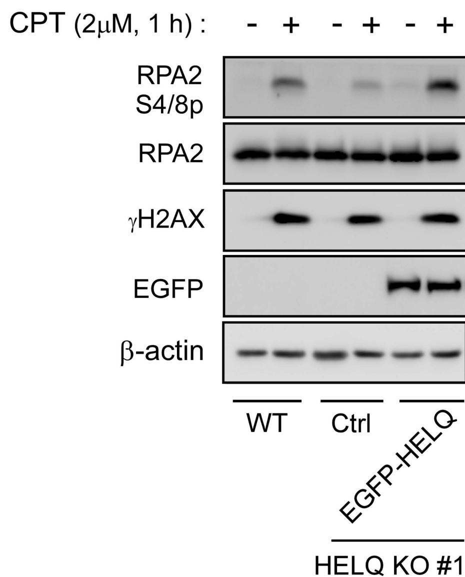

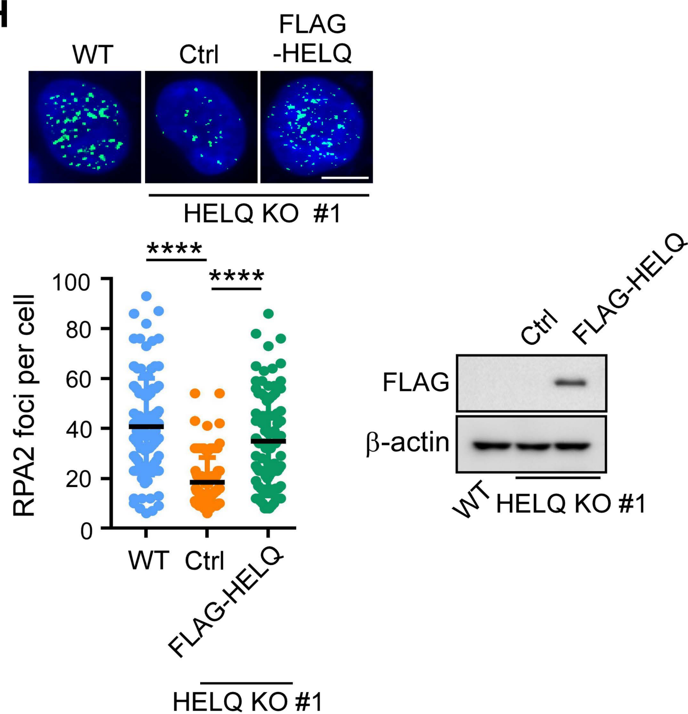

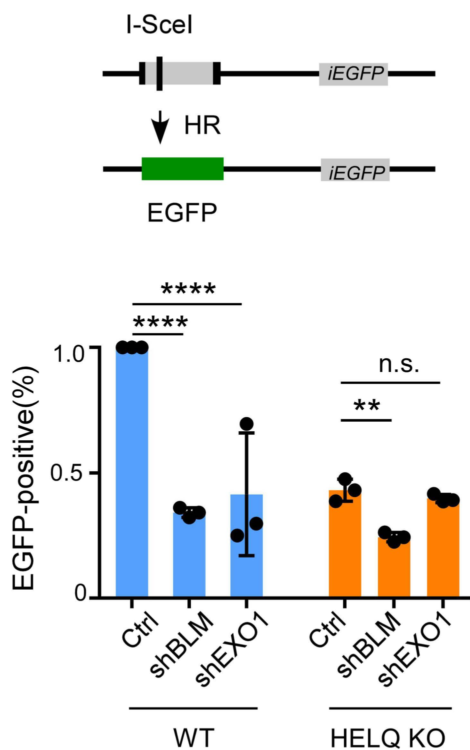

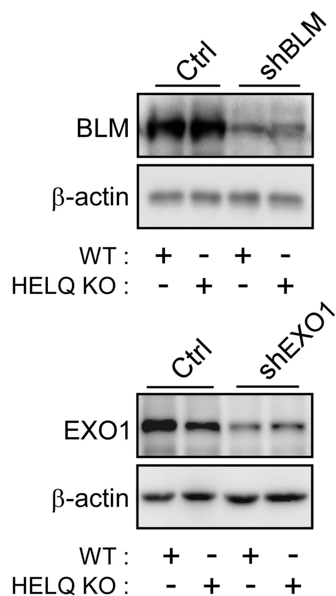

Continuation of Figure S2

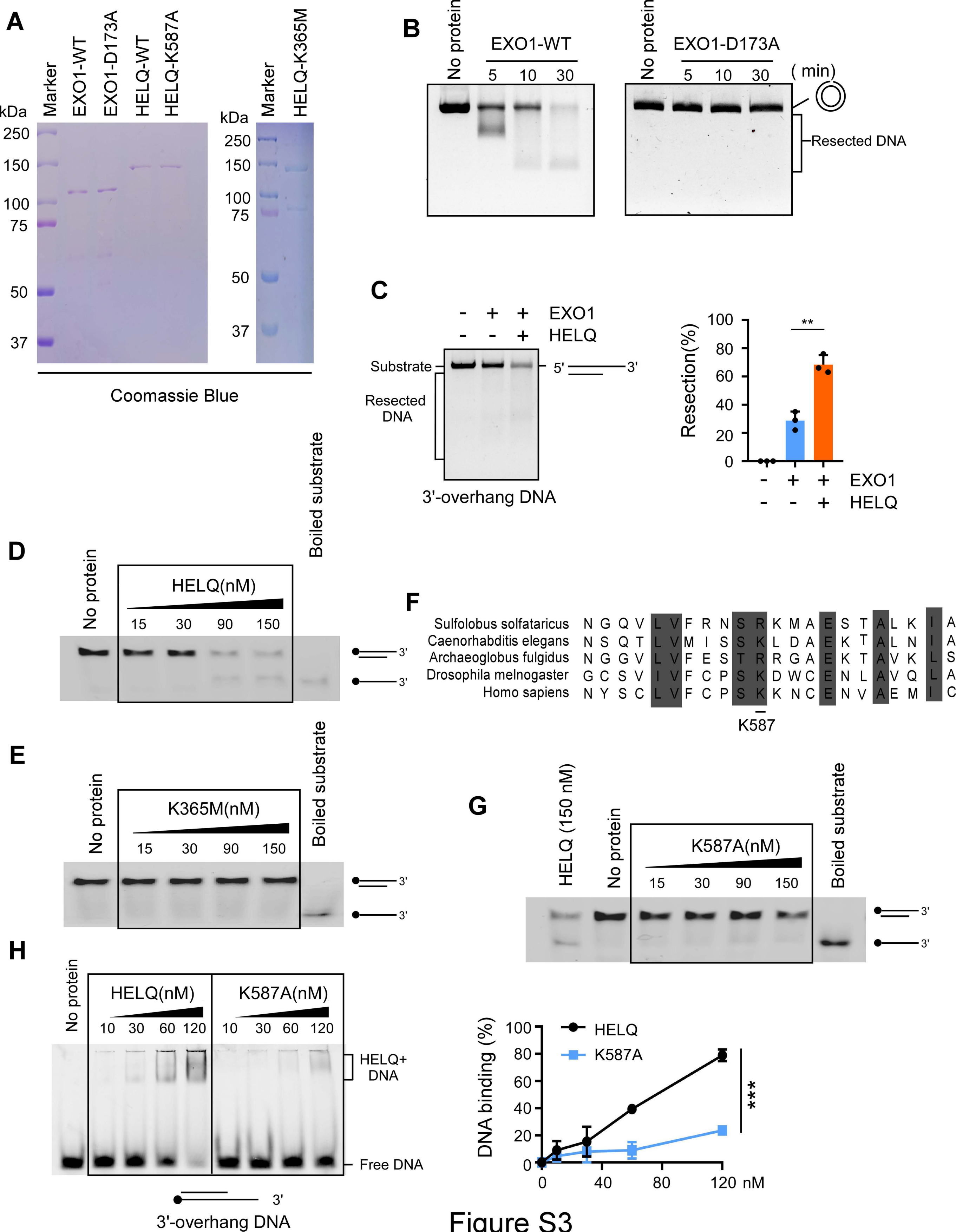

Figure S3

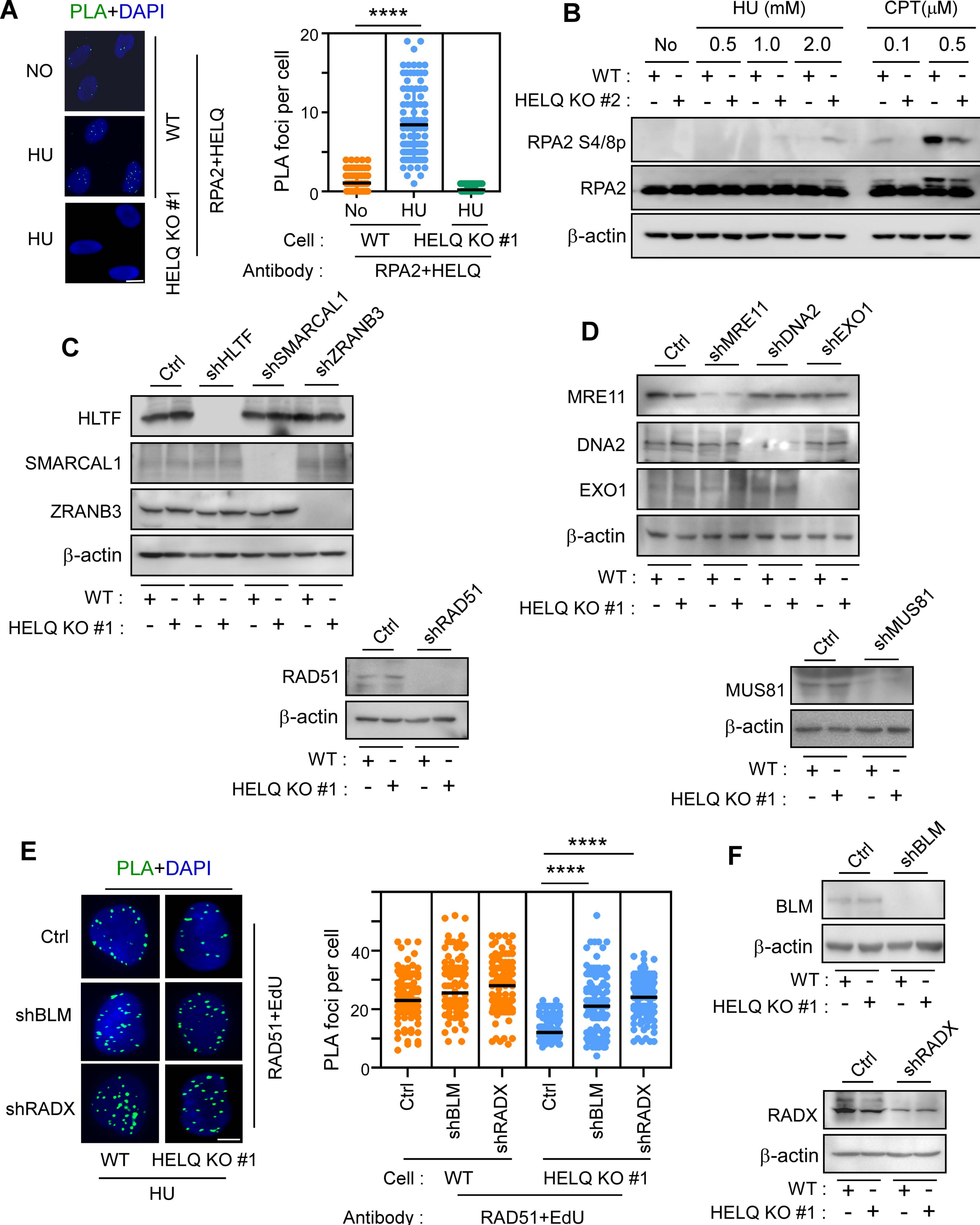

Figure S4

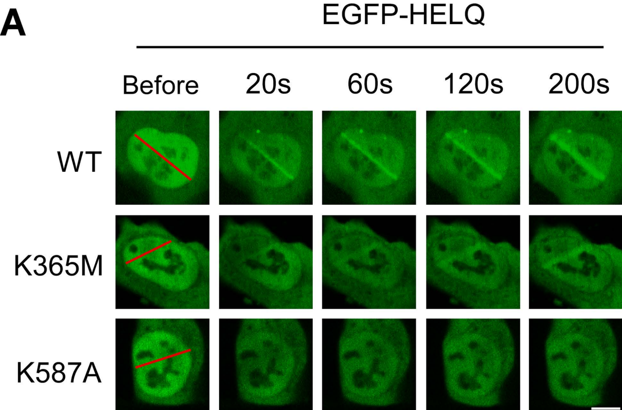

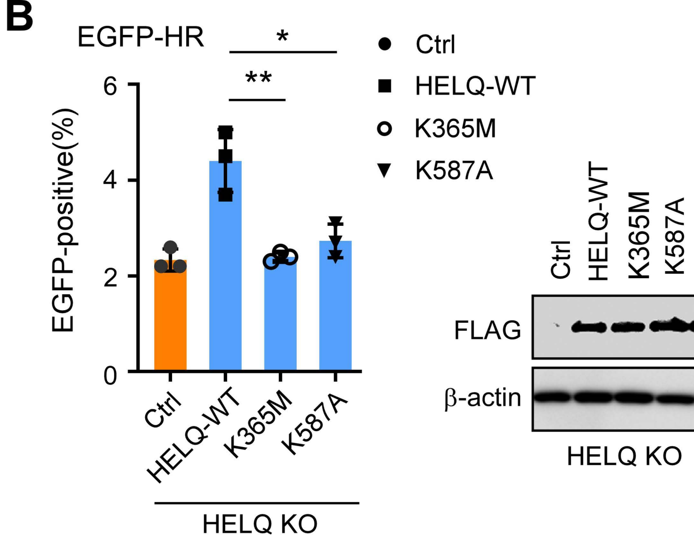

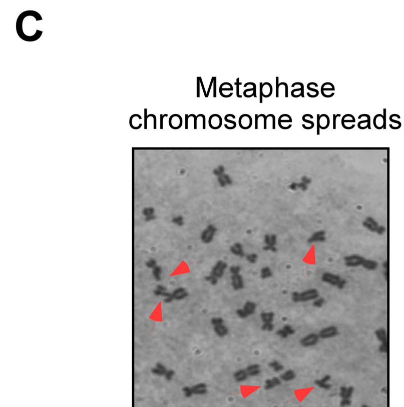

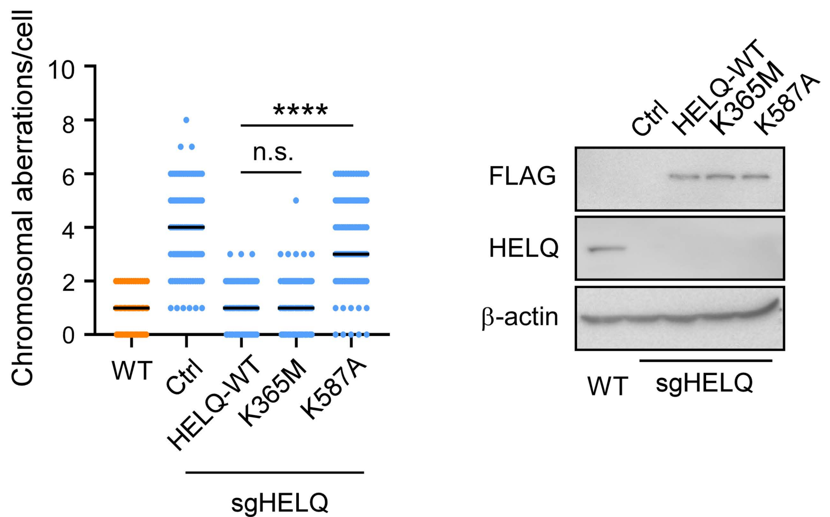

Figure S5

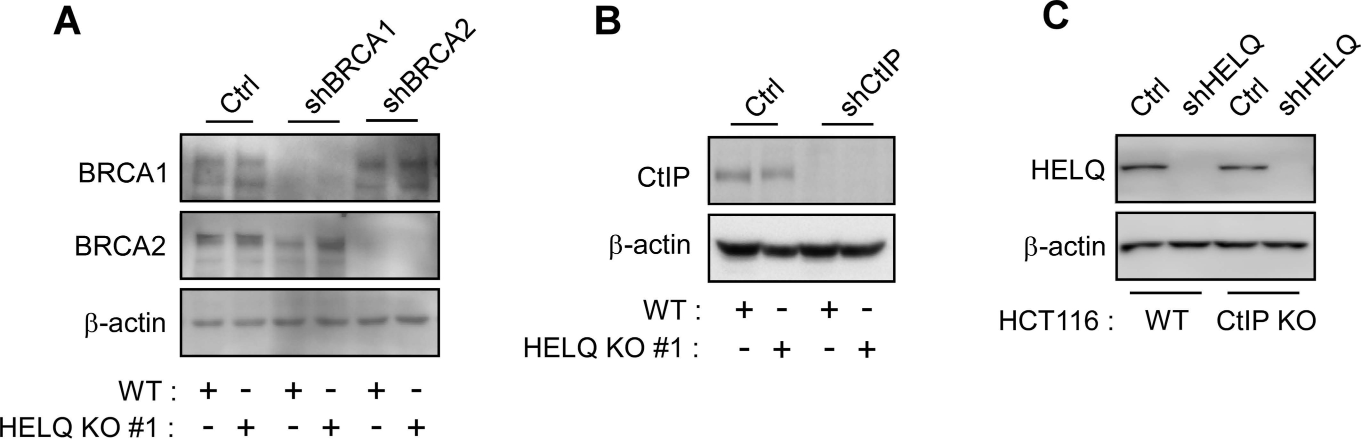

Figure S6